RSC Advances

ROYAL SOCIETY OF CHEMISTRY

www.rsc.org/advances

RSC Advances

ARTICLE

One-step Synthesis of Ni_3S_2 Nanoplatelets on Graphene for High Performance Supercapacitors

Received 00th January 20xx,
Accepted 00th January 20xx

DOI: 10.1039/x0xx00000x

www.rsc.org/

Xuewu Ou, Zhengtang Luo*

Here, we present a one-step hydrogen reduction synthesis of Ni_3S_2 nanoplatelets on graphene surface by using $NiSO_4{\cdot}3N_2H_4$/GO as precursor. In this process, we have demonstrated that hydrazine molecule, which can coordinate with $NiSO_4$ in the form of pink precipitation, not only contributes to the formation of Ni_3S_2 nanoplatelets structure, but also enhances the efficiency of SO_4^{2-} to S_2^{4-} conversion compared with $NiSO_4$/GO. Supercapacitors made from the obtained Ni_3S_2/rGO composite exhibits a specific capacitance of 912.2 F g^{-1} at 2 mV s^{-1} scanning rate, and 875.6 F g^{-1} at galvanostatic discharge current density of 1 A g^{-1}, along with exceptional rate capability of 83.2 % at discharge current density from 1 A g^{-1} to 10 A g^{-1} as well as good cycling stability. We attribute the excellent performance from the improved contact between graphene and the planar Ni_3S_2 structure, which strengthens the synergistic effect with graphene as conductive support and Ni_3S_2 nanoplatelets as the pseudocapacitive materials. This method allows the direct and efficient preparation of Ni_3S_2, and provides a simple route to integrate them with graphene for energy storage applications.

Introduction

Transition metal oxides and chalcogenides have been intensively studied because of their broad application such as energy storage and catalyst.[1-3] Among transition metal chalcogenides (TMCs), recently, Ni_3S_2 has attracted tremendous attention ascribed to their superior performance in energy storage. For example, it was reported that Ni_3S_2 nanorods prepared via hydrothermal method exhibits a specific capacitance of 1277 F g^{-1} at 2 mV s^{-1} scanning rate.[4] Similar method is used to produce $Ni_xCo_{3-x}S_4$ hollow nanoprisms, which also perform enhanced pseudocapacitive behavior.[5] However, those methods relies on wet chemistry through the sulfidation of Ni using H_2S decomposed from sulfur-containing molecules like thioacetamide (TAA) or thiourea that used in work mentioned above. Other methods like CVD method have also been reported, but the process involve many different steps thus are less efficient.[6]

On the other hand, due to the semiconducting property of TMCs, conductive materials like carbon materials are commonly used to combine with TMCs to improve their electron conductivity in order to fully exploit their pseudocapacitive capacity for energy storage application. However, to composite TMCs with carbon materials through wet chemistry is not efficient since transition metal nanoparticles should be integrated with the desired carbon materials firstly. Previously, we have developed a two-step method to prepare graphene supported droplet-shape structure of hollow Ni_3S_2/rGO and core-shell Ni@Ni_3S_2/rGO for supercapacitors application.[7] Although enhanced pseudocapacitance has been achieved, the process is still not easy enough.

In this work, we have further developed a direct method to prepare Ni_3S_2 nanoplatelets through H_2 reduction of $NiSO_4$-hydrazine complex ($NiSO_4{\cdot}3N_2H_4$). In addition, this method allows the convenient integration of Ni_3S_2 nanoplatelets with graphene through one-step H_2 reduction of $NiSO_4{\cdot}3N_2H_4$/GO. Compared with wet chemistry through the sulfidation of transition metals adopted elsewhere, this presented method shows several obvious advantages. Firstly, Ni_3S_2 are reduced directly from $NiSO_4{\cdot}3N_2H_4$, with no need to prepare nickel nanoparticles in advance as common methods. Secondly, Ni_3S_2 prepared from this method can be easily integrated with carbon materials like graphene avoiding the prior preparation of nickel/carbon material composites. Moreover, because of the interaction between Ni^{2+} and oxygen-containing groups on graphene oxide, the prepared Ni_3S_2 nanoplatelets have good contact with graphene, enabling charge transfer between them. After made into electrodes and tested for supercapacitors, a specific capacitance of 912.2 F g^{-1} at scanning rate of 2 mV s^{-1} and 875.6 F g^{-1} at 1 A g^{-1} galvanostatic discharge current density are obtained for Ni_3S_2/rGO composite reduced from $NiSO_4{\cdot}3N_2H_4$/GO. Compared with the two-step method we developed before,[7] the main advantage of this presented method is the simple process but comparable performance.

Department of Chemical and Biomolecular Engineering, Hong Kong University of Science and Technology, Clear Water Bay, Kowloon, Hong Kong. E-mail: keztluo@ust.hk

† Electronic supplementary information (ESI) available: The calculation method for specific capacitance, XRD, XPS, Raman, TEM and electrochemical test results.

Results and discussion

We have firstly investigated the hydrogen reduction of $NiSO_4$ and $NiSO_4{\cdot}3N_2H_4$, respectively. Here, $NiSO_4{\cdot}3N_2H_4$ is prepared according to previous reported method,[8] and the corresponding XRD result is shown in Fig. S1. During hydrogen reduction process, $NiSO_4{\cdot}7H_2O$ and $NiSO_4{\cdot}3N_2H_4$ are separately loaded into a furnace under 200 sccm Ar and 20 sccm H_2 at 400 ℃ for 2 h. After hydrogen reduction, as shown in XRD results in Fig. S2, peaks at 21.8° (101), 31.2° (110), 37.9° (003), 44.5° (202), 49.7° (211), 55.3° (300) of Ni_3S_2 (JCPDS no. 44-1418) are identified for both $NiSO_4{\cdot}7H_2O$ and $NiSO_4{\cdot}3N_2H_4$, suggesting the formation of Ni_3S_2 and the successful conversion of SO_4^{2-} into S_2^{4-}, and peaks at 51.9° (200), 76.5° (220) of Ni (JCPDS no. 04-0850) indicates partial reduction of Ni ions in $NiSO_4$ or Ni_3S_2 under H_2 environment. In a control experiment without introduction of H_2, after loading $NiSO{\cdot}7H_2O$ into furnace annealed under argon at 400 ℃ for 2h, only peaks for $NiSO_4$ are observed (Fig. S3), indicating that H_2 is a crucial reactant in this conversion. X-ray photoelectron spectroscopy (XPS) is then used to demonstrate the state change of sulphur element. From high resolution S2p XPS spectrum, after H_2 reduction of $NiSO_4{\cdot}3N_2H_4$, peak at range of 167 eV ~ 172 eV corresponding to SO_4^{2-} has been almost vanished along with the appearance of a new peak for S_2^{4-} at range of 160.5 eV ~ 163.5 eV in Figure 1,[9,10] indicating a complete conversion of SO_4^{2-} into S_2^{4-}. While using $NiSO_4{\cdot}7H_2O$ as precursor, besides the new peak for S_2^{4-}, high intensity SO_4^{2-} peak at range of 167 eV ~ 172 eV (Fig. S4) is still observed. Compared with $NiSO_4{\cdot}7H_2O$, it can be concluded that N_2H_4 indeed enhances the conversion of SO_4^{2-} to S_2^{4-} in $NiSO_4{\cdot}3N_2H_4$. Previous methods to realize such conversion relies on the use of sulphate-reducing bacteria (SRB), a type of anaerobic microorganisms, for sulphate degradation,[11] however, hydrogen reduction of transition metal sulphate or transition metal sulphate-hydrazine complex has not been reported before. At current stage, the conversion mechanism of $NiSO_4$ and $NiSO_4{\cdot}3N_2H_4$ into Ni_3S_2 is not clear. A possible explanation is that under H_2 environment at 400 ℃, Ni^{2+} and SO_4^{2-} will be reduced to Ni and H_2S/SO_2, respectively, followed by reaction between them to form Ni_3S_2.[7,12,13] Since the precursor $NiSO_4$ is water-soluble, the method we have developed here makes the convenient integration of Ni_3S_2 with carbon materials possible.

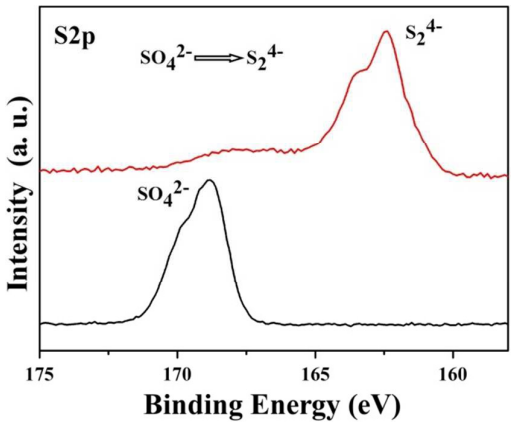

Figure 1. High-resolution S2p XPS spectrum of pure $NiSO_4$ (black line) and Ni_3S_2 reduced from $NiSO_4{\cdot}3N_2H_4$ by H_2 (red line).

To integrate Ni_3S_2 with graphene for supercapacitors application, Figure 2 displays the scheme for the preparation of Ni_3S_2/rGO from $NiSO_4{\cdot}3N_2H_4$/GO. In detail, firstly, $NiSO_4$/GO (Figure 2a) is prepared by simply mixing $NiSO_4$ solution with graphene oxide (GO) dispersion. After the observation of well mixing of $NiSO_4$ with GO, excess N_2H_4 solution is added dropwise. The key reason we use N_2H_4 here is that it can precipitate $NiSO_4$ in the form of $NiSO_4{\cdot}3N_2H_4$. Ascribed to electrostatic interaction between Ni^{2+} and oxygen-containing group on GO, the formed $NiSO_4{\cdot}3N_2H_4$ is supposed to sedimentate *in situ* and attach tightly onto graphene surface as shown in Figure 2b. After that, through one-step H_2 reduction of $NiSO_4{\cdot}3N_2H_4$/GO, Ni_3S_2/rGO are obtained and denoted as Ni_3S_2/rGO-2 (Figure 2c), and the XPS result is shown in Fig. S5, in which N element is detected due to the usage of N_2H_4. In another experiment, Ni_3S_2/rGO reduced directly from $NiSO_4$/GO by H_2 is denoted as Ni_3S_2/rGO-1. Figure 3 shows the XRD results of Ni_3S_2/rGO-1 and Ni_3S_2/rGO-2. Besides peaks for Ni_3S_2, graphene peak C(002) is also identified, confirming the

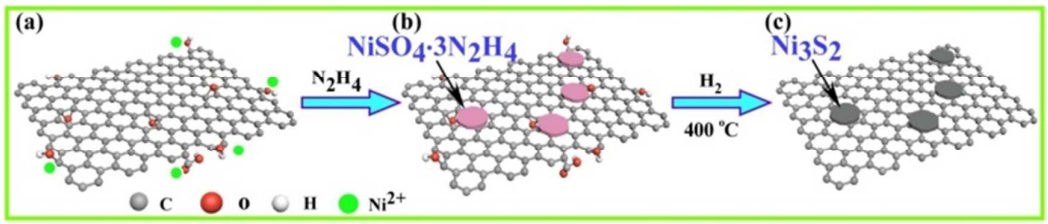

Figure 2. Schematic illustration for the synthesis of Ni_3S_2/rGO. (a) graphene oxide (GO) and Ni^{2+} aqueous solution. (b) $NiSO_4$ precipitates in the form of $NiSO_4{\cdot}3N_2H_4$ on GO after the introduction of hydrazine. (c) Ni_3S_2 nanoplatelets formed *in situ* on graphene surface after H_2 reduction, accompanied with the reduction of GO into rGO.

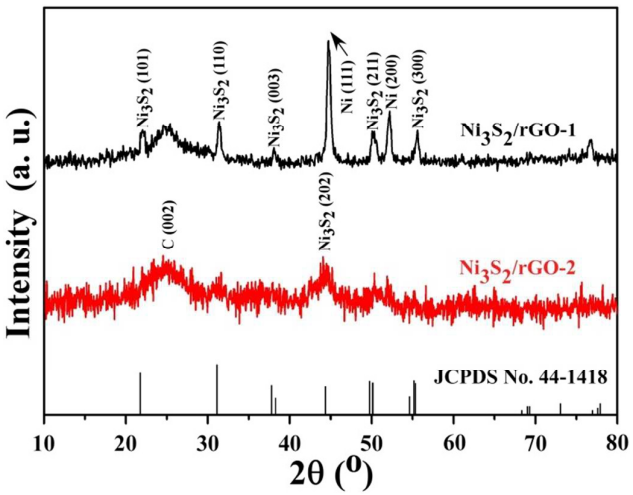

Figure 3. XRD spectrum of Ni_3S_2/rGO-1 reduced by H_2 from $NiSO_4$/GO and Ni_3S_2/rGO-2 reduced from $NiSO_4 \cdot 3N_2H_4$/GO, respectively.

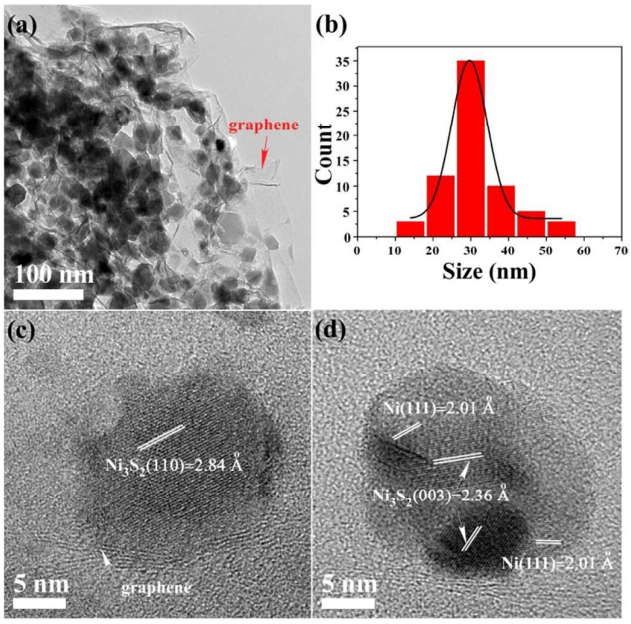

Figure 4. TEM results of Ni_3S_2/rGO reduced from $NiSO_4 \cdot 3N_2H_4$/GO. (a) Ni_3S_2 nanoplatelets with uniform size distributed on graphene surface. (b) Particle size analysis histogram of Ni_3S_2 nanoplatelets (mean: 29.6 nm, standard deviation: 9.4 nm). (c) and (d) High resolution TEM of Ni_3S_2 nanoplatelets on graphene surface.

successful integration of Ni_3S_2 with rGO. The lack of strong Ni_3S_2 diffraction peaks in sample Ni_3S_2/rGO-2 results from the well dispersion of Ni_3S_2 nanoplatelets on graphene surface as well as the small thickness of obtained Ni_3S_2 nanoplatelets, as confirmed by TEM results (shown later in Figure 4). Fig. S6 shows the Raman spectrum of GO in comparison with reduced graphene oxide in Ni_3S_2/rGO-1 and Ni_3S_2/rGO-2. The increase of I_D/I_G ratio from 0.733 (GO) to 1.051 for Ni_3S_2/rGO-1 and 1.066 for Ni_3S_2/rGO-2 indicates the reduction of GO.

Morphology of Ni_3S_2/rGO is characterized by transmission electron microscopy (TEM), and shown in Figure 4, for Ni_3S_2/rGO-2 (*i.e.* reduced from $NiSO_4 \cdot 3N_2H_4$/GO). We can see small nanoplatelets with uniform size are distributed on the graphene surface without obvious aggregation. In contrast, TEM images of Ni_3S_2/rGO-1 (*i.e.* reduced from $NiSO_4$/GO) show round and irregular nanoparticles with broad diameter distribution, as depicted in Fig. S7. The morphology difference observed should be resulted from the different precipitation process. In $NiSO_4$/GO, $NiSO_4$ deposits from solution and randomly anchors on the graphene surface during the drying-recrystallization process. On the contrary, for $NiSO_4 \cdot 3N_2H_4$/GO, with the aid of N_2H_4, $NiSO_4$ is precipitated in the form of $NiSO_4 \cdot 3N_2H_4$ and tightly fixed on the graphene surface due to the interaction between Ni^{2+} and oxygen-containing groups, similar to previous work for the preparation of $NiO/Ni(OH)_2$ nanosheets/nanoplates.[14,15] During the following H_2 reduction of $NiSO_4 \cdot 3N_2H_4$/GO, Ni_3S_2 will be prepared *in situ* to form Ni_3S_2/rGO, while Ni_3S_2 is more likely to aggregate into different morphology and size in Ni_3S_2/rGO-1 (*i.e.* reduced from $NiSO_4$/GO). From the particle size analysis histogram in Figure 4b, the average size of these Ni_3S_2 nanoplatelets is about 29.6 nm for Ni_3S_2/rGO-2. High resolution TEM image in Figure 4c shows the crystal structure, and plane spacing of 2.84 Å corresponds to Ni_3S_2 (300). More importantly, these Ni_3S_2 nanoplatelets are in good contact with graphene as pointed out by white arrow in Figure 4c, in agreement with our previous analysis. In addition, Ni domains from partial reduction of Ni ions in $NiSO_4/Ni_3S_2$ can be detected in some particles as illustrated in Figure 4d, consistent with XRD results stated before.

To demonstrate their potential application in energy storage, we further use electrochemical methods to investigate capacitive property of Ni_3S_2/rGO-1 (*i.e.* reduced from $NiSO_4$/GO) and Ni_3S_2/rGO-2 (*i.e.* reduced from $NiSO_4 \cdot 3N_2H_4$/GO), respectively. The electrochemical tests of those synthesized materials are carried out in a three-electrode setup, where Pt works as the counter electrode, Hg/HgO as the reference electrode and 2 M KOH as the electrolyte solution. Electrochemical results are shown in Figure 5, in which cyclic voltammetry (CV) test is conducted between 0.1 V and 0.6 V, and galvanostatic charge/discharge test range is from 0.1 V to 0.55 V. Figure 5a shows the CV curves for Ni_3S_2/rGO-1 and Ni_3S_2/rGO-2 at scanning rate of 2 mV s^{-1}, and both of these two composites show a pair of reversible redox peaks at the range between 0.25 V and 0.5 V, demonstrating their pseudocapacitive properties. And a specific capacitance of 360 F g^{-1} for Ni_3S_2/rGO-1 and 912.2 F g^{-1} for Ni_3S_2/rGO-2 can be calculated from these CV curves (for detailed calculation see the Supporting Information). CV

results at different scanning rate from 2 mV s^{-1} to 50 mV s^{-1} are presented in Fig. S8a and Fig. S8c for Ni_3S_2/rGO-1 and Ni_3S_2/rGO-2, respectively. Figure 5b displays the galvanostatic discharge curves at 1 A g^{-1}, and a specific capacitance of 140.0 F g^{-1} for Ni_3S_2/rGO-1 and 875.6 F g^{-1} for Ni_3S_2/rGO-2 are obtained (see the Supporting Information for calculation method). The significantly increased performance for Ni_3S_2/rGO-2 is possibly due to several reasons. Firstly, with the aid of N_2H_4, the conversion of SO_4^{2-} into S_2^{4-} is more complete, as confirmed with XPS result. Thus after H_2 reduction, $NiSO_4 \cdot 3N_2H_4$/GO leads to higher ratio of Ni_3S_2 active materials than that of $NiSO_4$/GO. Secondly, the Ni_3S_2 nanoplatelets in Ni_3S_2/rGO-2 have better contact with graphene substrate than round/irregular shape Ni_3S_2 nanoparticles with non-uniform size randomly deposited on graphene in Ni_3S_2/rGO-1. Thirdly, due to its highly reductive property, hydrazine can help reduce GO into rGO, contributing to improved electronic conductivity. Ni_3S_2/rGO-2 also delivers better rate capability than Ni_3S_2/rGO-1 as plotted in Figure 5c. By increasing galvanostatic charge/discharge current density from 1 A g^{-1} to 10 A g^{-1}, the calculated specific capacitance for Ni_3S_2/rGO-2 varies from 875.6 F g^{-1} to 728.5 F g^{-1}, equal to 83.2 % capacitance is retained. While for Ni_3S_2/rGO-1, specific capacitance decreases rapidly from 140 F g^{-1} to 42.2 F g^{-1}, only 30.1 % capacitance maintained. Fig. S8b and Fig. S8d present the galvanostatic discharge curves for these two composites at different current density from 1 A g^{-1} to 10 A g^{-1}. The CV and galvanostatic discharge curves for pure Ni_3S_2-2 reduced from $NiSO_4 \cdot 3N_2H_4$ and pure rGO are presented in Fig. S9, and a capacitance value of 333.8 F g^{-1} for Ni_3S_2-2 and 78.2 F g^{-1} for rGO are obtained at 1 A g^{-1} discharge current density. Taking into account the rGO weight percentage of 55.6%, the faradic capacitance is 832.1 F g^{-1} for Ni_3S_2/rGO-2 at 1 A g^{-1} current density. Electrochemical impedance spectroscopy (EIS) is also employed to measure the ion diffusion and charge transfer process at the frequency from 100 kHz to 10 mHz with amplitude of 5 mV, and results are shown in Nyquist plots in Figure 5d, with inset equivalent circuit, where *Rs* is the ohmic resistance accounting for the intrinsic resistance of electrode, contact resistance between current collector and electrode materials as well as the electrolyte resistance, C_{DL} is the double layer capacitance, R_{CT} is the charge transfer resistance, W is the Warburg diffusion element and C_F is the faradic capacitance.[7,16] The Nyquist plots fit well with the equivalent circuit by the equation:[16]

$$Z = R_s + \frac{1}{jwC_{DL} + \frac{1}{R_{CT} + W}} - \frac{j}{wC_F}$$

The lower *Rs* of 0.53 Ω for Ni_3S_2/rGO-2 than Ni_3S_2/rGO-1 (0.78 Ω) should be mainly resulted from its better conductivity due to the introduction of N_2H_4. The R_{CT} for Ni_3S_2/rGO-1 and Ni_3S_2/rGO-2 are 1.23 Ω and 1.01 Ω, respectively. Smaller R_{CT} value for Ni_3S_2/rGO-2 indicates better charge transfer, attributed to the good contact of Ni_3S_2 nanoplatelets with graphene. At last, we have conducted the cycling performance test for Ni_3S_2/rGO-2 (*i.e.* reduced from $NiSO_4 \cdot 3N_2H_4$/GO) at current density of 5 A g^{-1}, as shown in Fig. S10. After 1000 cycles at this current density, 91.3 % capacitance is maintained, demonstrating its good cycling stability.

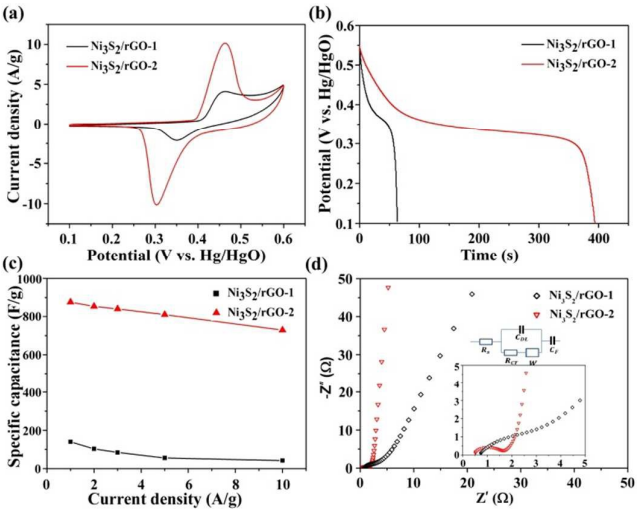

Figure 5. Electrochemical results of Ni_3S_2/rGO. (a) CV at scanning rate of 2 mV s^{-1} for Ni_3S_2/rGO reduced from $NiSO_4$/GO (Ni_3S_2/rGO-1) and $NiSO_4 \cdot 3N_2H_4$/GO (Ni_3S_2/rGO-2) respectively. (b) Corresponding galvanostatic discharge results at 1 A g^{-1} for Ni_3S_2/rGO-1 and Ni_3S_2/rGO-2. (c) Rate capability comparison of Ni_3S_2/rGO-1 and Ni_3S_2/rGO-2 at discharge current density from 1 A g^{-1} to 10 A g^{-1}. (d) Nyquist plots at amplitude of 5 mV over frequency range from 100 kHz to 0.01 Hz. Inset are the equivalent circuit and high frequency part zoomed in.

Experimental

Chemicals

Graphite (Grafguard 160-50N with the average particle size of 350 um) was expanded by microwave before use. $K_2S_2O_8$, P_2O_5, H_2SO_4, $KMnO_4$, H_2O_2, $NiSO_4 \cdot 7H_2O$, N_2H_4 (35 wt% in water) and poly(vinylidene fluoride)(PVDF) were all purchased from Sigma-Aldrich with analytical grade and used without further purification.

Preparation of graphene oxide (GO)

Graphene oxide (GO) is prepared through modified Hummers method.[17,18] In brief, firstly, 30 mL concentrated sulfuric acid is added into a flask containing 1 g graphite, 5 g $K_2S_2O_8$ and 5 g P_2O_5, reacted at 90 °C for 4.5 h. Then filtrate the product through a 0.2 micron Nylon Millipore filter and wash the sample with excess DI until the pH is around 5.5. Secondly, after drying the sample at 60 ℃, 150 mL concentrated sulfuric acid and 30 g $KMnO_4$ are added in sequential slowly and reacted at 35 ℃ for another 4 h. Thirdly, the mixture product is added to 1 L DI water and stirred for 2 h, followed by the addition of 50 mL 30 % H_2O_2 until the solution turns into bright yellow. After stirred for another 2 h, settle down the solution for 24 h. Finally, discard the supernatant and use 1 L of 10 %

HCl solution and excess DI to wash the product until the pH ~ 7.

Preparation of $NiSO_4 \cdot 3N_2H_4$ complex

To 2 ml 0.1 M $NiSO_4$ solution, 1 mL hydrazine solution (35 wt. % in H_2O) is added and stirred for 10 mins. After filtration and drying the pink precipitate, $NiSO_4 \cdot 3N_2H_4$ is obtained.

Preparation of $NiSO_4$/GO and $NiSO_4 \cdot 3N_2H_4$/GO composites

To 20 ml 1 mg/mL GO solution, 2 mL 0.1 M $NiSO_4$ is added slowly under vigorous stirring, and then stirred for another 1 h. After freeze-drying the mixture solution, $NiSO_4$/GO composite is obtained. To prepare $NiSO_4 \cdot 3N_2H_4$/GO composite, 1 mL hydrazine solution (35 wt. % in H_2O) is added into the above $NiSO_4$/GO solution. After filtration and drying the product, $NiSO_4 \cdot 3N_2H_4$/GO composite is obtained.

Preparation of Ni_3S_2/rGO composites

Load the prepared $NiSO_4$/GO and $NiSO_4 \cdot 3N_2H_4$/GO composite into a furnace under 200 sccm Ar and 20 sccm H_2 at 400 ℃ for 2h, respectively. After cooling down to room temperature, the products are collected. rGO and Ni_3S_2 are prepared separately through a procedure similar to the preparation of Ni_3S_2/rGO, apart from the absence of $NiSO_4$ and GO respectively. The mass ratio of Ni_3S_2 in Ni_3S_2/rGO-1 and Ni_3S_2/rGO-2 are 63.1% and 55.6%, respectively.

Crystal structure and morphology characterization:

All the characterization tests are done in Materials Characterization and Preparation Facility (MCPF) in Hong Kong University of Science and Technology (HKUST). XRD (PW1830, Philips) with Cu Kα radiation (λ=1.5406 Å) is used to test the phase structure. The state change of sulphur is checked with XPS (VG Micro Tech ESCA 2000). And transmission electron microscope (TEM, JEOL 2010) is used to characterize the morphology and crystal structure.

Electrode preparation and electrochemical measurement:

90 wt% electrode materials and 10 wt% PVDF as the binder are put into an agate mortar to make slurry. Then coat the slurry onto Ni foam with area of 1 cm^2 uniformly. After drying at 80 ℃ for 12 h under vacuum environment, the prepared electrodes are pressed tightly under 10 MPa. Three-electrode system is employed here to measure the electrochemical properties of the electrodes. In this system, the prepared electrode is used as the working electrode, platinum plate as counter electrode and Hg/HgO as reference electrode. The electrolyte used here is 2 M KOH. Before the electrochemical test, the electrodes are dipped into the electrolyte for 6 h. The electrochemical test is carried out on an electrochemical workstation (CHI 660). Cyclic voltammetry test and galvanostatic charge/discharge test are conducted at the range from 0.1 V to 0.6 V and 0.1 V to 0.55 V, respectively. The electrochemical impedance spectroscopy (EIS) is done at the frequency range from 100 kHz to 0.01 Hz under amplitude of 5 mV.

Conclusions

In summary, we have synthesized Ni_3S_2 directly from $NiSO_4$-hydrazine complex ($NiSO_4 \cdot 3N_2H_4$) through H_2 reduction, and integrated these Ni_3S_2 nanoplatelets with graphene for supercapacitors application. As a result, Ni_3S_2/rGO reduced from $NiSO_4 \cdot 3N_2H_4$/GO shows a specific capacitance of 912.2 F g^{-1} at scanning rate of 2 mV s^{-1} and 875.6 F g^{-1} at 1 A g^{-1} discharge current density. We believe that hydrazine molecule introduced in $NiSO_4 \cdot 3N_2H_4$ contributes to the enhancement of conversion of SO_4^{2-} into S_2^{4-}, and also allows the formation of Ni_3S_2 nanoplatelets, ensuring better contact with the underlying graphene. The method presented here provides a new simple route for the preparation of Ni_3S_2 as well as Ni_3S_2/rGO composite for energy storage.

Acknowledgements

This project is supported by the Research Grant Council of Hong Kong SAR (Project number 623512 and DAG12EG05). Technical assistance from the Materials Characterization and Preparation Facilities is greatly appreciated.

Notes and references

(1) Jiang, J.; Li, Y.; Liu, J.; Huang, X.; Yuan, C.; Lou, X. W. D. *Advanced Materials* **2012**, *24*, 5166.
(2) Wachs, I. E. *Catalysis Today* **2005**, *100*, 79.
(3) Kong, D.; Cha, J. J.; Wang, H.; Lee, H. R.; Cui, Y. *Energy & Environmental Science* **2013**, *6*, 3553.
(4) Zhou, W.; Cao, X.; Zeng, Z.; Shi, W.; Zhu, Y.; Yan, Q.; Liu, H.; Wang, J.; Zhang, H. *Energy & Environmental Science* **2013**, *6*, 2216.
(5) Yu, L.; Zhang, L.; Wu, H. B.; Lou, X. W. D. *Angewandte Chemie* **2014**, *126*, 3785.
(6) Lin, R.; Hu, D.; Chang, Y. *Metallurgical Transactions B* **1978**, *9*, 531.
(7) Ou, X.; Gan, L.; Luo, Z. *Journal of Materials Chemistry A* **2014**, *2*, 19214.
(8) Li, Y.; Li, C.; Wang, H.; Li, L.; Qian, Y. *Materials chemistry and physics* **1999**, *59*, 88.
(9) Liao, Y.; Pan, K.; Pan, Q.; Wang, G.; Zhou, W.; Fu, H. *Nanoscale* **2015**, *7*, 1623.
(10) Legrand, D. L.; Nesbitt, H. W.; Bancroft, G. M. *American Mineralogist* **1998**, *83*, 1256.
(11) Muyzer, G.; Stams, A. J. *Nature Reviews Microbiology* **2008**, *6*, 441.
(12) Zhou, W.; Chen, W.; Nai, J.; Yin, P.; Chen, C.; Guo, L. *Advanced Functional Materials* **2010**, *20*, 3678.
(13) Gilewicz-Wolter, J. *Oxidation of metals* **1988**, *29*, 225.
(14) Zhou, G.; Wang, D.-W.; Yin, L.-C.; Li, N.; Li, F.; Cheng, H.-M. *Acs Nano* **2012**, *6*, 3214.
(15) Wang, H.; Casalongue, H. S.; Liang, Y.; Dai, H. *Journal of the American Chemical Society* **2010**, *132*, 7472.
(16) Choi, B. G.; Hong, J.; Hong, W. H.; Hammond, P. T.; Park, H. *ACS nano* **2011**, *5*, 7205.

(17) Hummers, W. S. O., R. E. *Journal of the American Chemical Society* **1958**, *80*, 1339.
(18) Luo, Z.; Lu, Y.; Somers, L. A.; Johnson, A. C. *Journal of the American Chemical Society* **2009**, *131*, 898.

One-step Synthesis of Ni_3S_2 Nanoplatelets on Graphene for High Performance Supercapacitors

Xuewu OU, Zhengtang LUO*

Department of Chemical and Biomolecular Engineering, Hong Kong University of Science and Technology, Clear Water Bay, Kowloon, Hong Kong

E-mail: keztluo@ust.hk

A one-step hydrogen reduction synthesis of Ni_3S_2 nanoplatelets on graphene surface has been developed for supercapacitors application.